Engineering Structures 34 (2012) 233–243

Contents lists available at SciVerse ScienceDirect

Engineering Structures

journal homepage: www.elsevier.com/locate/engstruct

A numerical study of the seismic behaviour of timber shear walls with slip-friction connectors

Wei Y. Loo *, Pierre Quenneville, Nawawi Chouw

Department of Civil and Environmental Engineering, Faculty of Engineering, University of Auckland, Private Bag 92019, Auckland Mail Centre, Auckland 1142, New Zealand

ARTICLE INFO

Article history:
Received 19 August 2010
Revised 9 September 2011
Accepted 10 September 2011
Available online 4 November 2011

Keywords:
Shear walls
Hysteresis behaviour
Slip-friction
Energy dissipation
Ductility
Timber structures

ABSTRACT

In the event of seismic overloading, timber shear walls have normally been designed to yield by allowing inelastic distortion of the sheathing-to-framing nail connections, thereby reducing the likelihood of brittle failure of timber chords or plywood sheathing. A new concept in shear wall design is presented. It involves the use of slip-friction connectors in lieu of traditional hold-down connectors. Slip-friction connectors, originally developed for the steel framing industry, rely on the mobilisation of friction across steel plates to resist loading up to a predetermined threshold. Upon this threshold being exceeded, relative sliding between the steel plates allows the shear wall to displace in an inelastic manner. This paper discusses the results of numerical analyses of timber shear walls which utilise slip-friction connectors. The results suggest that slip-friction connectors hold the promise of being able to effectively protect sheathing, framing, and nail connections from excessive stresses and deformations during earthquake events of design level intensity or higher. Walls with appropriately adjusted slip-friction connectors are highly ductile, are efficient dissipaters of seismic energy, and have a tendency to self-centre after an earthquake.

1. Introduction

The use of wood as a construction material has seen significant increase in recent years, not only in low level residential buildings, but also in the construction of multi-storey buildings.

Timber shear walls are widely used to provide lateral force resistance for timber-framed buildings. During an earthquake, timber shear walls are normally designed to behave in a ductile manner [1]. The sheathing to framing nail connections yield and deform inelastically, shielding the framing and sheathing from brittle failure, whilst at the same time maintaining the lateral strength of the wall and dissipating energy. Through this process, the shear walls, whilst being expected to perform their life preserving duty of preventing catastrophic collapse, will nevertheless incur substantial post-earthquake residual damage [2].

An innovation which could significantly mitigate this post-earthquake residual damage to walls, and also allow for self-centring of walls immediately after an earthquake, is to replace the traditionally used hold-down anchors, which prevent overturning of the wall, with a type of semi-rigid steel joint – the slip-friction connector.

Slip-friction connectors, unlike the hold-down anchors currently used ('traditional' connectors), allow vertical slip displacement upon a pre-defined force threshold being exceeded. Slip-friction connectors, through the principle of moment equilibrium, can thus limit the size of horizontal forces on shear walls (see Fig. 1(a)).

With careful design, the intention is that the desired ductile behaviour and energy dissipation characteristics that timber shear walls already exhibit is maintained, or even improved upon – but the inelastic deformations which allow this to take place are instead concentrated at the slip-friction connectors, thereby relieving the sheathing-to-framing nailed connections of this duty, and thus avoiding permanent damage to the wall.

Sliding friction devices were originally developed for use in earthquake resistant steel structures. Seminal research was carried out by Popov et al. [4] on the feasibility of using sliding steel plates as energy dissipaters, and Clifton et al. [5] has developed a 'sliding hinge' connector specifically for beam to column joints in steel frames. Butterworth [6] describes the use of slip-friction connectors in concentrically braced steel frames.

For timber structures, Filiatrault [7] has investigated the use of similar friction devices implemented at all four corners of shear walls. Such a set-up was found to effectively limit inertia forces on the walls, as well as mitigate inelastic damage. Duff et al. [8] has carried out experimental work on the use of slip-friction devices in timber T-connections. Favourable results were obtained, with the T-connections exhibiting highly desirable hysteretic characteristics, along with negligible degradation of strength and stiffness under cyclic loading.

* Corresponding author. Tel.: +64 9 3737599x83512; fax: +64 9 3737462.
E-mail addresses: wloo002@aucklanduni.ac.nz (W.Y. Loo), p.quenneville@auckland.ac.nz (P. Quenneville), n.chouw@auckland.ac.nz (N. Chouw).

0141-0296/$ - see front matter © 2011 Elsevier Ltd. All rights reserved.
doi:10.1016/j.engstruct.2011.09.016

Notation

B	wall width
C	compression force
CSP	Canadian softwood plywood
F	force on wall, nail connection or slip-friction connector
F_{slip}	slip threshold force of slip-friction connector
F_{ult}	ultimate strength of shear wall or nail connection
F_y	yield strength of shear wall or nail connection
H	wall height
LVL	laminated veneer lumber
MCE	maximum credible earthquake
n_b	number of bolts
OSB	oriented strand board
PGA	peak ground acceleration
SPF	spruce pine fir
T	tension force
T_b	tension in bolt
ULS	ultimate limit state
V	base shear
W	weight of wall
μ	overall wall ductility as defined by δ_{fail}/δ_y
μ_{fr}	coefficient of friction
μ_{SF}	that part of overall wall ductility contributed by maximum possible slippage of slip-friction connector
δ	lateral displacement of a shear wall or nail connection
δ_{fail}	displacement of shear wall corresponding to 0.8 F_{ult}, on the degrading portion of the force-displacement curve
δ_s	that part of overall wall displacement due to maximum possible slippage of slip-friction connector
δ_{ult}	displacement at ultimate strength, F_{ult}, of shear wall or nail connection
δ_y	displacement at yield force, F_y, of shear wall or nail connection

For pre-cast concrete walls, Bora et al. [3] carried out tests using slip-friction connectors as hold-down anchors. The results have been promising, with the connectors successfully limiting loads on the tested walls and providing ductility to these otherwise brittle systems. The slip-friction connector adopted by Bora et al. is shown in Fig. 1(b).

This paper describes a numerical study into the effectiveness of using slip-friction connectors as hold-down anchors for timber shear walls, in order to reduce the impact of earthquakes on timber structures.

2. Modelling of slip-friction connectors

2.1. Description

The slip-friction connector envisioned for implementation in timber shear walls will be similar in concept to the configuration successfully tested in pre-cast concrete walls [3].

The slip-friction connector of Fig. 1(b) consists of brass plates, or shims, which clamp down on either side of a slotted centre plate. These in turn are bolted between a cover plate and a wall-embedded plate.

Vertical forces from the wall are transferred to the wall-embedded plate, and the reaction force from the ground is applied to the foundation-embedded plate. No external force is applied directly to the cover plate. The cover plate serves only to clamp the assemblage together and maintain the normal force necessary to mobilise static friction amongst the plates. In the event of the mobilised friction forces being exceeded, the wall-embedded plate will slide relative to the centre plate, and the cover plate will be 'dragged' along by the bolt/s in the direction of the wall-embedded plate. This type of sliding is called asymmetric sliding, and is better illustrated by Fig. 1(c).

Asymmetric sliding contrasts with the case of symmetric sliding, where an external force is applied to a slotted centre plate, with the two outside plates each providing one half of the reaction against the external force.

The slip threshold, F_{slip}, of the mechanism of Fig. 1(c) is given by Eq. (1).

$$F_{slip} = 2n_b T_b \mu_{fr} \tag{1}$$

2.2. Modelling the force–displacement behaviour of slip-friction connectors

In order to model the force–displacement behaviour of slip-friction connectors, three types of finite element are used. These are the multi-linear plastic link, the gap, and the hook. The multi-linear plastic link is used to provide the desired elasto-plastic behaviour of a slip-friction connector. There are various hysteresis types available for the multi-linear plastic link. The kinematic hysteresis type, which does not allow stiffness degradation, is selected.

During slippage of the plates the stiffness of the connector is zero, and the connector provides a constant resisting force of F_{slip}. Unloading and reloading is modelled to always take place in a linear fashion, with the gradient (stiffness) of the unloading and

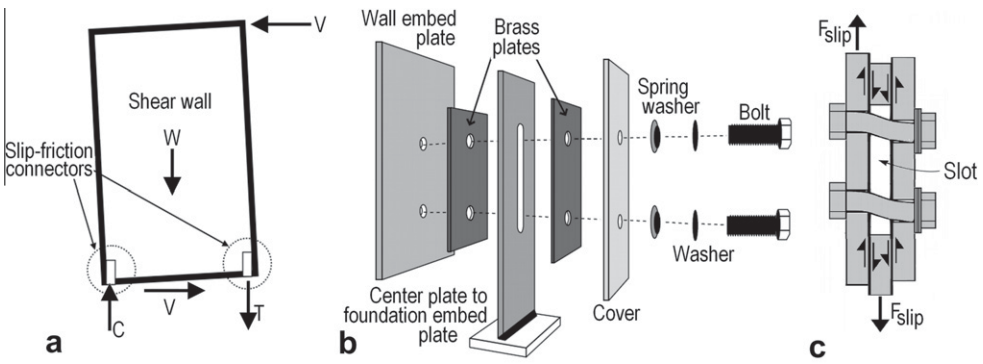

Fig. 1. Slip-friction connectors with shear walls: (a) capping of lateral force on shear wall, (b) connector assemblage for pre-cast concrete wall (courtesy of the Precast/Prestressed Concrete Institute [3]), and (c) activated friction forces.

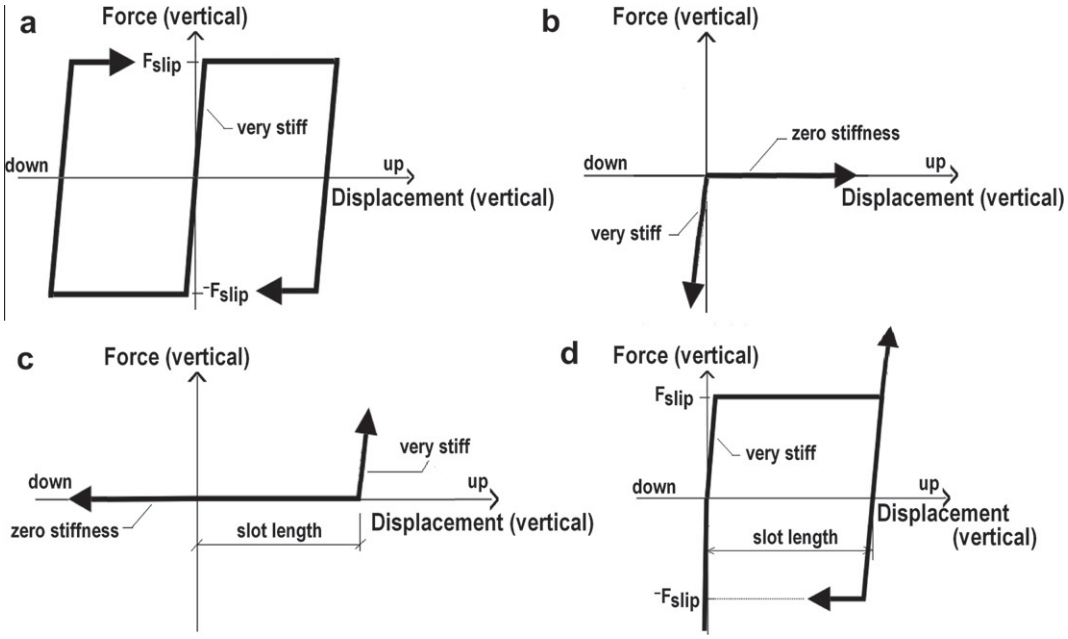

Fig. 2. Slip-friction connector behaviour: Force–displacement relationship of (a) multi-linear plastic link element, (b) gap element, (c) hook element, and (d) slip-friction force–displacement relationship as combination of multi-linear plastic link, gap and hook elements.

reloading lines remaining unchanged, regardless of loading history (Fig. 2(a)).

The multi-linear plastic link element, by itself, would allow displacement both upwards and downwards. But in reality, the bottom corner of the shear walls to which the slip-friction connectors attach, cannot displace below the level of their original position. Thus, the slip-friction connector limits negative displacement to essentially zero. This is achieved by the gap element. The initial 'gap' of the gap element is set to zero i.e. the gap is closed until an upward force is applied to the element. The force–displacement relationship of the gap element is defined so that any downward displacement will be negligible (Fig. 2(b)).

The next aspect to consider is the maximum allowable uplift displacement. At the slip-friction connector location, the upward displacement would be limited by the length of the slot through which the bolt/s clamping the plates together, move. The slot can be modelled using a hook element (Fig. 2(c)).

The three elements mentioned above, combine together to produce the overall force–displacement relationship of the slip-friction connector (Fig. 2(d)).

The slip-friction connector so modelled is included at the bottom corners of shear walls.

3. Modelling shear walls with slip-friction connectors

3.1. Overview of modelling process

A simplified method was developed by the authors for the numerical modelling of timber shear walls. The modelling procedure, using SAP2000 [9], is briefly described in this section.

Timber shear walls typically comprise sheathing material (normally plywood or oriented strand board) nailed to timber framing. The timber framing supports gravity loads. The end studs of the framing provide most of the resistance to overturning moments on the wall. The sheathing prevents lateral deformation of the framing. The overall behaviour of the timber shear wall is largely governed by the nonlinear behaviour of the sheathing-to-framing nail connections [10].

For relatively small displacements in which P-delta effects and other nonlinearities are not expected to arise, a good representation of shear wall behaviour can be produced by modelling nonlinear behaviour at the nail connections only, whilst ignoring all possible nonlinear behaviour in the sheathing or framing materials.

To model nail elements, a multi-linear plastic link element is used. This element, as already discussed, is also used as part of the slip-friction connector assemblage. However, to model nail behaviour, the pivot hysteresis type is selected, rather than the kinematic hysteresis type used to model slip-friction connectors. The pivot hysteresis type has parameters to control strength and stiffness degradation during the entire loading, thereby allowing the pinching effect typically observed for nail connections under cyclic loading to be reproduced.

The force–displacement behaviour of nails is derived from empirical data and mechanics based analytical assumptions which take into account sheathing, framing, and nail properties. Fig. 3 compares the numerically obtained force–displacement relationship for 3 mm model nails with the experimental result [11].

Fig. 4 shows a model wall with slip friction connectors. Frame elements are used to model the timber studs and bottom plate and top plates. Sheathing (shaded area in Fig. 4) is modelled using shell elements, with only membrane actions considered. Nail elements attach the sheathing to framing; their locations are coincident with nodes on the meshed sheathing. The numerical model is verified using data obtained from experiments by other researchers [12].

The displacement-control spring of Fig. 4 allows a time history of displacement loading to be applied to the wall. This linear spring obviates numerical convergence problems post-ultimate loading of the shear wall.

Fig. 5 shows the numerically obtained hysteretic behaviour of a 2.4×2.4 m model shear wall with traditional connectors, and compares this with the result obtained from the loading of an equivalent actual wall. The result for the actual wall was provided by Dr. M. Popovski of FPInnovations, Canada (personal communication, December 1, 2008). The modelled wall is of 9.5 mm thick CSP sheathing connected by 3 mm diameter nails (spaced at

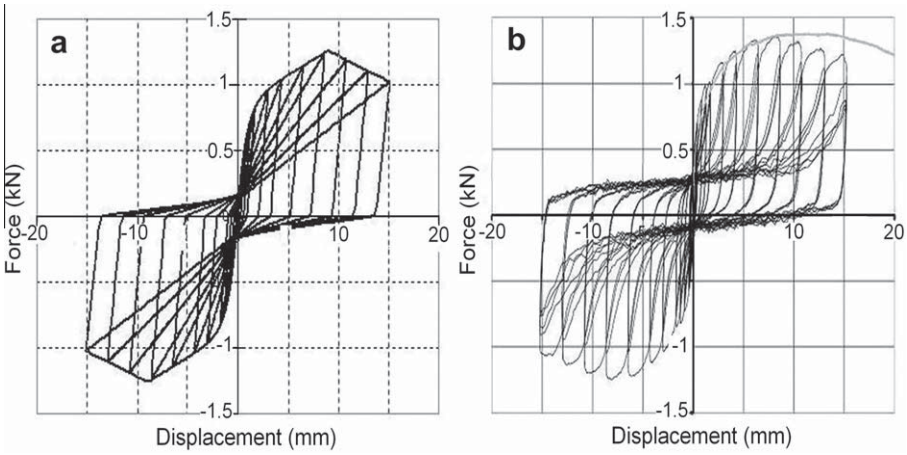

Fig. 3. Three millimeter nails connecting 11 mm OSB sheathing to SPF framing: (a) numerical response. (b) experimental response (courtesy of Dinehart [11]).

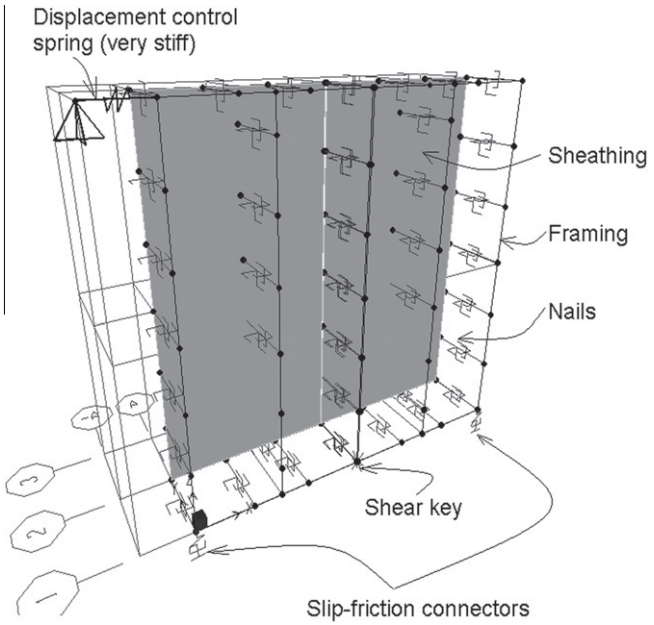

Fig. 4. Shear wall setup.

150 mm) to 38 × 89 mm SPF framing lumber. Studs are spaced at 406 mm centre to centre.

3.2. Determining connector slip threshold

Deciding on a rational method for the determination of the yield force, F_y, of a shear wall with traditional hold-down connections is important in the design and modelling of timber shear walls with slip-friction connectors. This is because the purpose of the slip-friction connector is to limit the lateral force on the timber shear wall to be no greater than F_y. In this way the wall will be protected from inelastic material damage of sheathing, framing, and nail connections when coming under lateral loading.

The way in which the yield force is determined for the shear walls modelled in this paper is shown in Fig. 6(a).

From Fig. 6(a) the yield force, F_y is defined as half that of F_{ult}. Also shown is the determination of the failure displacement δ_{fail}.

Assuming the yield force to be half the ultimate lateral strength has been recommended by Munoz et al. [14]. In addition to this, numerical analyses carried out by the authors on a range of model shear walls confirms that the 50% rule for calculating yield force produces values which align very closely with design strengths calculated according to NZS3603 [13] (see Fig. 6(b)).

For the modelling of shear walls with slip-friction connectors, the connector slip threshold, F_{slip}, is set so that slippage will occur when the laterally applied force at the top of the wall (for monotonic and slow cyclic loading) is equal to F_y. Using a static equilibrium analysis of the wall, F_{slip} is calculated from Eq. (2).

$$F_{slip} = \frac{F_y H}{B} - \frac{W}{2} \tag{2}$$

3.3. Wall ductility and connector slot length

The ductility of a wall is typically defined in reference to the maximum displacement and the yield displacement (Eq. (3)).

$$\mu = \delta_{fail}/\delta_y \tag{3}$$

However, another measure of ductility suggested by the authors is μ_{SF}, which relates directly to the maximum uplift (equates to slot length) allowed by the slip friction connector at the bottom corner of a wall – see Fig. 7.

From Fig. 7 it can be seen that the overall contribution to wall ductility from the slip-friction connector is given by Eq. (4).

$$\mu_{SF} = \frac{H \times (\text{slot length})}{B\delta_y} + 1 \tag{4}$$

By rearranging Eq. (4), the slot length is found from Eq. (5).

$$\text{slot length} = B\delta_y(\mu_{SF} - 1)/H \tag{5}$$

Note that μ_{SF} is important because it represents the connector contribution to the ductility the wall can achieve without significant inelastic damage. Note that the total ductility of the wall, μ, will always be higher than μ_{SF}. If the wall is displaced to such an extent that the slot end of the slip-friction connector is impacted upon, the connector becomes incapable of limiting the lateral force applied to the wall. With increasing displacement, the mobilised wall resistance will increase to the ultimate strength of the wall, and with still further displacement the failure displacement is eventually reached. It is this failure displacement, δ_{fail}, which Eq. (3) uses to determine the total wall ductility, μ.

3.4. Walls under cyclic load

The configuration of the model wall to be studied numerically under cyclic loading is given in Table 1.

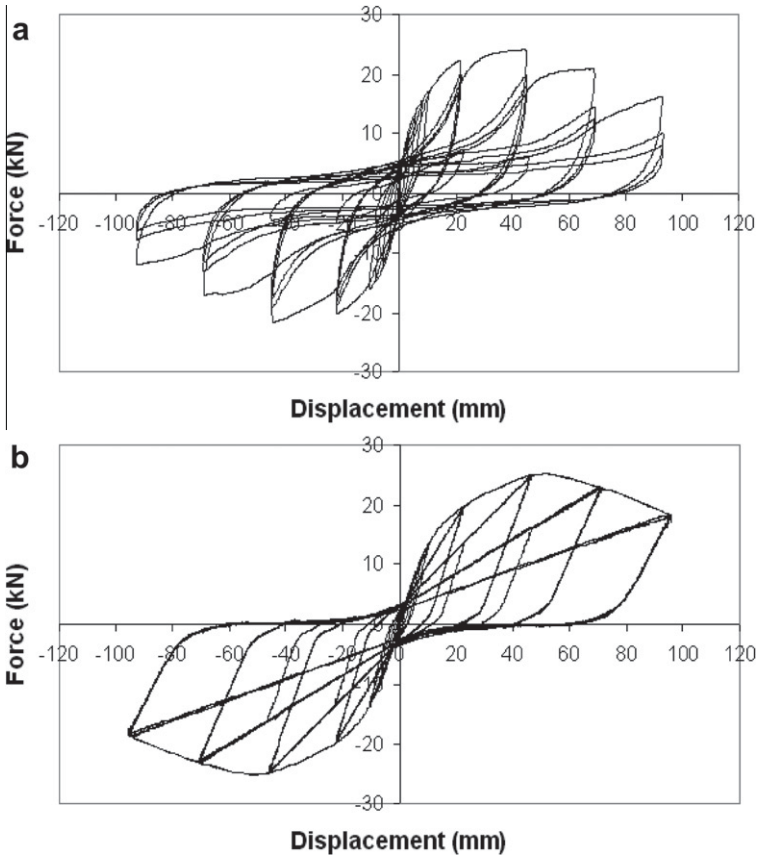

Fig. 5. Force–displacement behaviour of 2.4 × 2.4 m wall: (a) experimentally obtained (courtesy of Dr. M. Popovski at FPInnovations, Canada) compared with (b) numerically obtained.

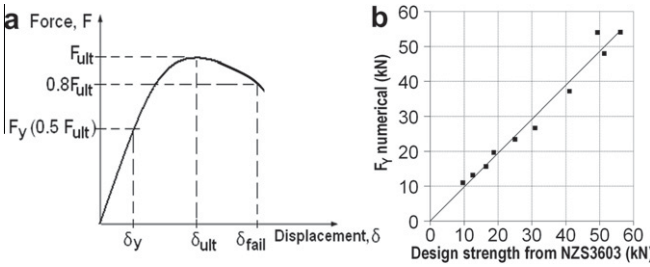

Fig. 6. Shear wall yield force F_y: (a) determination of F_y and failure displacement δ_{fail} and (b) numerically obtained $F_y = 0.5\,F_{ult}$ and design strength according to NZS3603 [13].

A version of the numerical model of a wall with traditional hold-down connectors was first analysed. Then the same model wall, with slip-friction connectors in lieu of traditional hold-downs was considered three additional times – each time with a longer slot. The ISO97 displacement time history was used for all the numerical simulations (see Fig. 8a). This displacement loading is described in [12]. The loading rate was 20 mm/s. The maximum displacement used was 100 mm, which corresponds to a drift of 4% for 2.44 m tall walls.

The displacement loading of Fig. 8(a) was first applied to the wall with traditional connectors. The resulting force–displacement relationship is shown in Fig. 8(b). It can be seen that the wall incurs significant inelastic deformation. The force–displacement behaviour of the model wall displays the classic 'pinching' behaviour associated with actual timber shear walls under cyclic loading. The wall's ultimate strength, F_{ult}, is 22 kN. Using the 50% rule, the yield force $F_y = 11$ kN. The associated yield displacement of

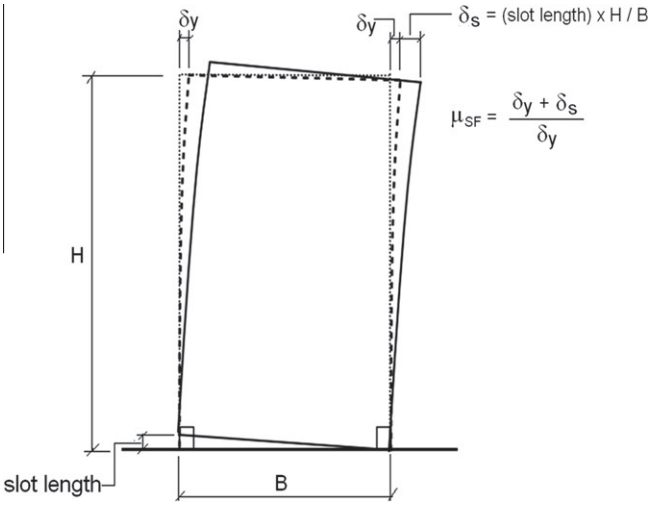

Fig. 7. Relationship between slot length and wall displacement.

$\delta_y = 9$ mm, is obtained from the envelope curve to the hysteresis loops.

With slip-friction connectors, the slip threshold (also taking into account wall weight) was set at $F_{slip} = 10.5$ kN (from Eq. (2)). Walls with slip-friction connectors were considered at three different slot lengths to give $\mu_{SF} = 2$, 4, and 6, respectively. From Eq. (5), the corresponding values for slot lengths are 9 mm, 27 mm, and 45 mm.

The behaviour of the wall with a slot length of 9 mm ($\mu_{SF} = 2$) is shown in Fig. 8(c). It is clear that the effect of the connector has re-

Table 1
Wall properties.

Wall property	Value
Overall dimensions (m)	2.44 × 2.44
Number of panel rows	1
Number of panel columns	2
Plywood sheathing thickness (mm)	9
Plywood, elastic modulus, E (MPa)	10,500
Plywood, shear modulus, G (MPa)	525
F11 ply, density (kg/m^3)	560
LVL end-chords dimensions (mm)	90 × 45
LVL, elastic modulus, E (MPa)	13,200
LVL, density (kg/m^3)	620
Stud spacings (mm)	600
Nail diameter & spacings (mm)	2.8 diameter @ 150
Weight of wall, W (kN)	1.0

sulted in some reduction of the 'pinching' effect (compare with force–displacement relationship of Fig. 8(b)).

Note that as the displacement increases, the stiffness of the wall deteriorates, and the 'plateau' effect of the force–displacement relationship gradually becomes less evident, as the strength of the wall reduces to below that provided by the connector slip threshold. The displacement at peak strength is offset however, by a distance close to that of the length of the slip-friction induced 'plateau'.

Fig. 8(d) shows the performance of the wall with connector slot length increased to 27 mm. The hysteresis loops are further 'fattened', with a displacement at ultimate strength, δ_{ult} of 76 mm (compared to 50 mm for the wall with traditional hold-down connectors).

Fig. 8(e) shows the wall behaviour with slip-friction connector slot lengths increased still further, to 45 mm. The 'fat' loops indicative of ideal elasto-plastic behaviour now clearly dominate.

The energy dissipation of the walls is found by calculating the total area bounded by the hysteresis loops. Cumulative energy dissipation is plotted against time for each of the considered walls (Fig. 9(a)).

From Fig. 9(a), it can be seen that the rate of energy dissipation is significantly influenced by varying the slot length of the slip-friction connectors. The wall with connector slot length of 45 mm ($\mu_{SF} = 6$), dissipated energy at a rate 1.7 times higher than that of the same wall with traditional connectors.

In Fig. 9(b), the forces in the end-chords of the wall with traditional connectors, are compared with the same for the wall with slip-friction connectors of 45 mm ($\mu_{SF} = 6$) slot length. It can be seen that applying slip-friction connectors to the wall limits the maximum force on the end-chords to about 8.3 kN. 8.3 kN is

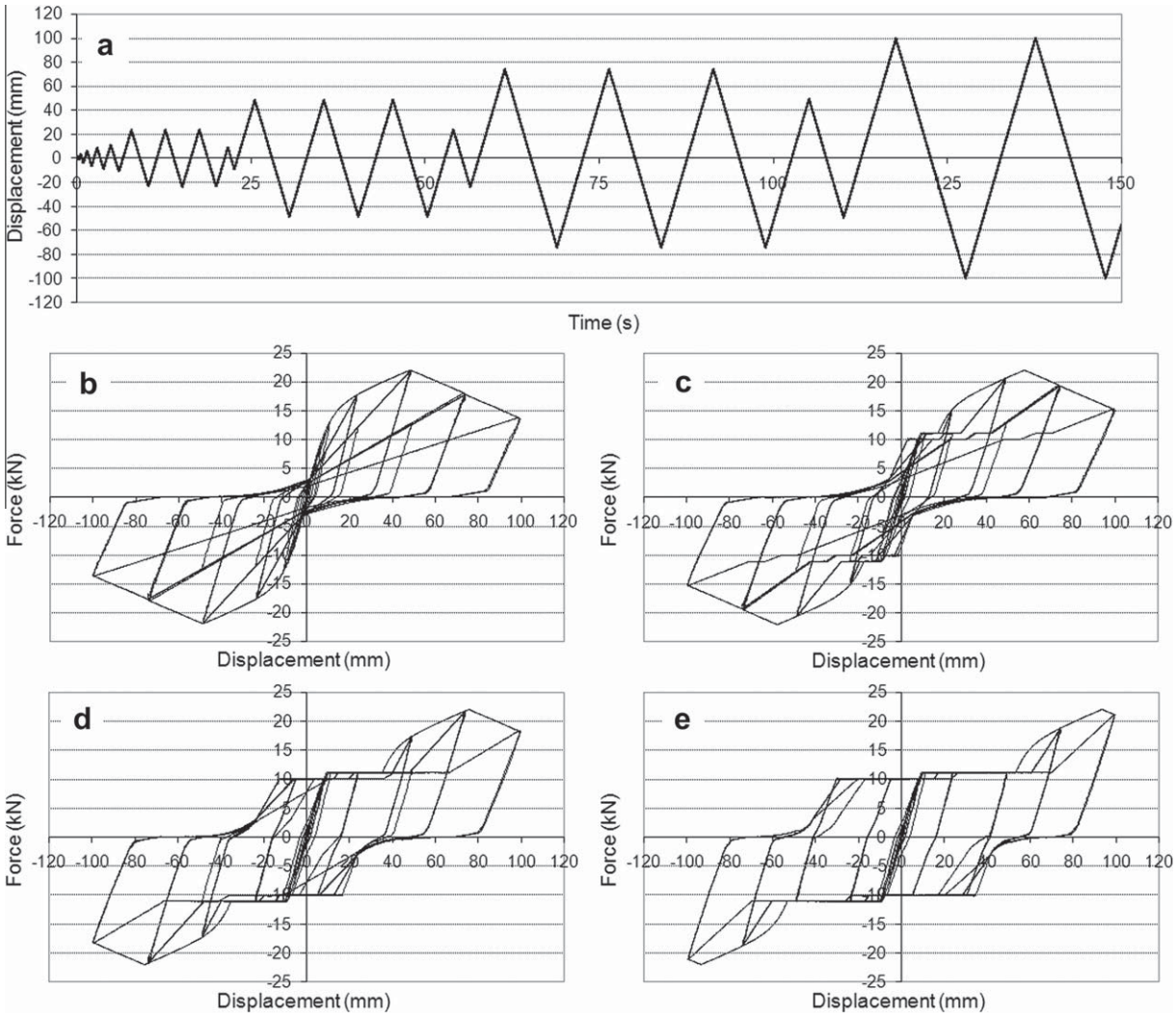

Fig. 8. Cyclic response of 2.44 × 2.44 m wall: (a) displacement time history; hysteretic behaviour of wall with (b) traditional hold-downs; (c) slip-friction connectors of 9 mm slot length ($\mu_{SF} = 2$) and (d) 27 mm slot length ($\mu_{SF} = 4$) and (e) 45 mm slot length ($\mu_{SF} = 6$).

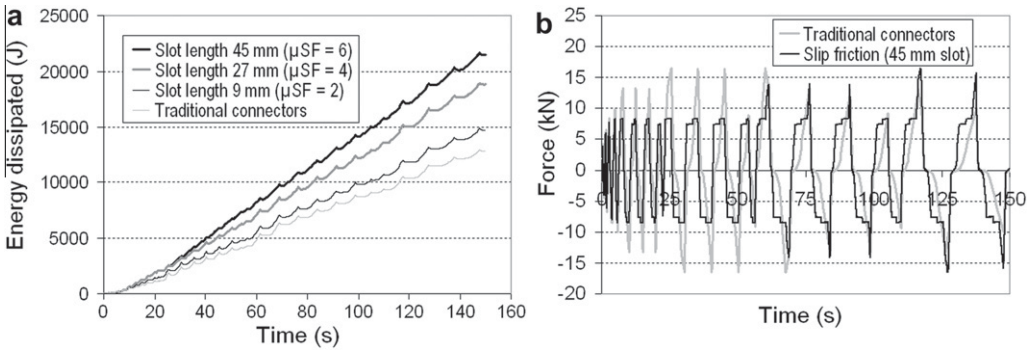

Fig. 9. Slip-friction connector effect on wall under cyclic loading: (a) energy dissipation and (b) activated end-chord forces (positive and negative values are tension and compression, respectively).

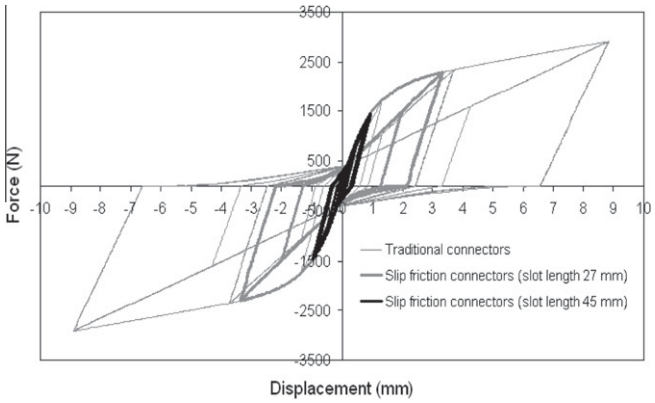

Fig. 10. Force–displacement relationships of nail element at top corner of shear wall during first 60 s of loading. Note that one nail element is used to represent four actual nail connections.

consistent with a slip-friction connector force threshold of 10.5 kN (the discrepancy exists because the reaction provided by the connectors will not be transferred to only the end-chords – a minor part of this force will transfer to the interior studs via the sheathing which is nailed to the timber framing). Later into the loading the tension and compression forces in the end-chords peak at about 16.4 kN – at this loading stage, the bolts of the connector can impact the slot ends, and the activated end-chord forces will increase to beyond the capped value associated with connector sliding.

Similar observations can also be made in the development of sheathing shear stresses (not presented here). Shear stresses are capped when slip-friction connectors are used in lieu of traditional connectors.

Fig. 10 shows the hysteretic behaviour of a nail connection at one of the top corners of the shear wall. With traditional connectors, the nail incurs significant inelastic deformation. However with increasing wall ductility provided by the slip-friction connectors, the level of inelastic damage to the observed nail connection is significantly reduced.

4. Earthquake loading

4.1. Setup of model walls

The model timber shear walls were subjected to earthquake loadings of various intensities. The response of walls with slip-friction connectors is compared to that of walls with traditional hold-down connectors.

The configuration used for the walls was similar to that used for cyclic loading (see Table 1), the only differences being studs spaced at 400 mm (not 600 mm), and 2.5 mm diameter nails spaced at 170 mm (not 2.8 mm @ 150 mm spacings). To enhance computational efficiency one model nail was used to represent four actual nails. A mass of 8000 kg was assigned to the top of the wall to simulate the upper four stories of a five-storey light timber frame building.

For walls with slip-friction connectors, F_{slip} was determined as follows: From monotonic loading of the model wall with traditional connectors, F_{ult} was found to be 16.7 kN. Using the 50% rule F_y = 8.4 kN (with corresponding yield displacement δ_y = 7.6 mm). The weight of the wall was 1 kN. From Eq. (2), F_{slip} = 7.9 kN. Slot lengths were set as unlimited.

Five commonly used earthquake acceleration records were selected for earthquake loading (see Table 2).

The 5% damped spectra associated with each of the earthquake records were scaled to match the Hamilton 500 year return period (ULS – ultimate limit state) and 2500 year return period (MCE – maximum considered earthquake) target spectra for Type C (intermediate) soils. Scale factors were calculated in accordance with NZS1170 [16], using the numerically determined fundamental wall frequency of 2.2 Hz.

The resulting scaled peak ground accelerations for the earthquake records are shown in Table 3.

Walls with and without slip friction connectors were considered for each of the five earthquakes, at two different limit states.

Table 2
Earthquake records.[a]

Event	Station	Direction	PGA (g)
Imperial Valley (El Centro), 1940	117 El Centro Array #9	N–S	0.313
Loma Prieta, 1989	47125 Capitola	E–W	0.529
Northridge, 1994	24303 LA – Hollywood Stor	E–W	0.231
Kobe, 1995	0 KJMA	N–S	0.821
Landers, 1992	22170 Joshua Tree	E–W	0.284

[a] From Pacific Earthquake Engineering Research Center [15].

Table 3
Earthquake testing – scaled peak ground acceleration.

Event	Scaled PGA for ULS (g)	Scaled PGA for MCE (g)
El Centro, 1940	0.16	0.25
Loma Prieta, 1989	0.11	0.24
Northridge, 1994	0.14	0.25
Kobe, 1995	0.16	0.25
Landers, 1992	0.17	0.31

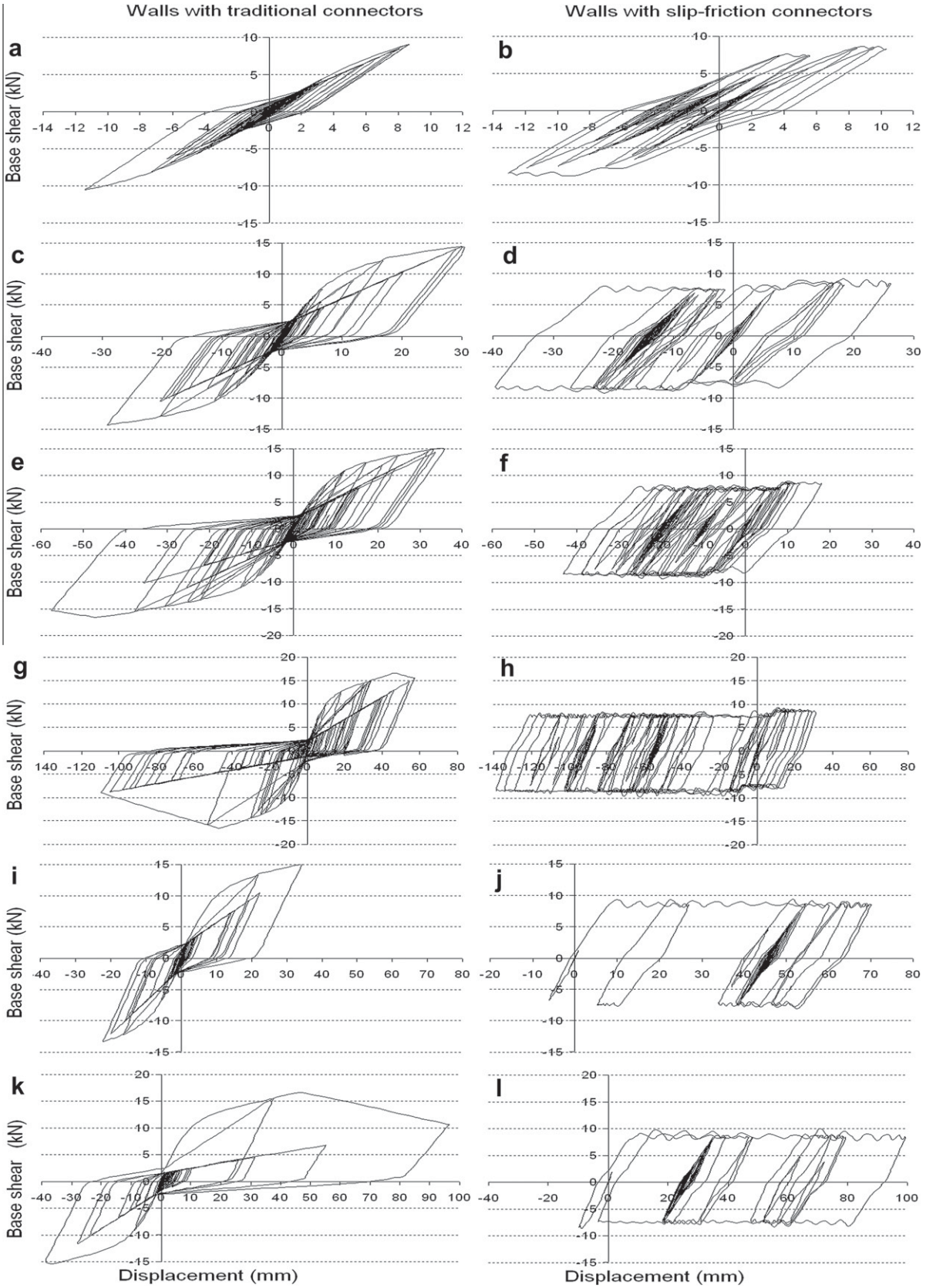

Fig. 11. Force–displacement responses to Loma Prieta ULS event with (a) traditional connectors and (b) slip-friction connectors; Loma Prieta MCE event with (c) traditional connectors and (d) slip-friction connectors; Landers ULS event with (e) traditional connectors and (f) slip-friction connectors; Landers MCE event with (g) traditional connectors and (h) slip-friction connectors; Kobe ULS event with (i) traditional connectors and (j) slip-friction connectors; Kobe MCE event with (k) traditional connectors and (l) slip-friction connectors.

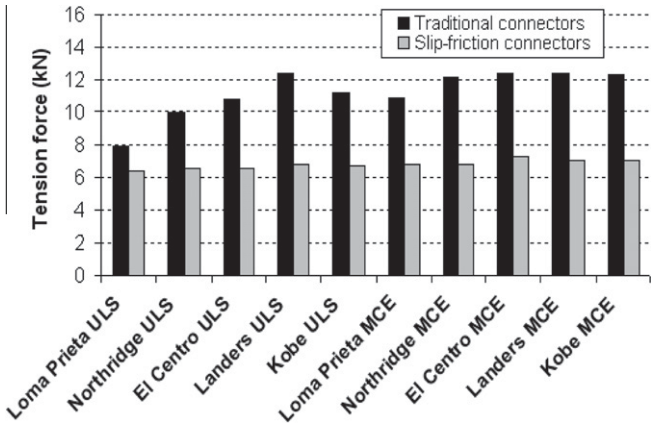

Fig. 12. Earthquake loading: end-chord tension forces.

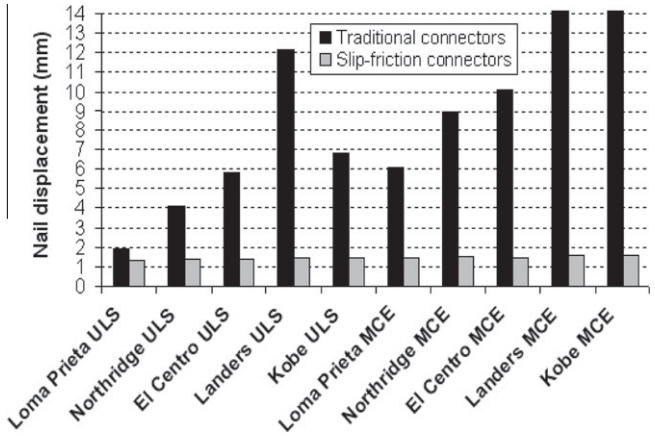

Fig. 13. Earthquake loading: nail connection displacements (*note:* total displacements for Landers MCE and Kobe MCE, 26 mm and 22 mm, respectively).

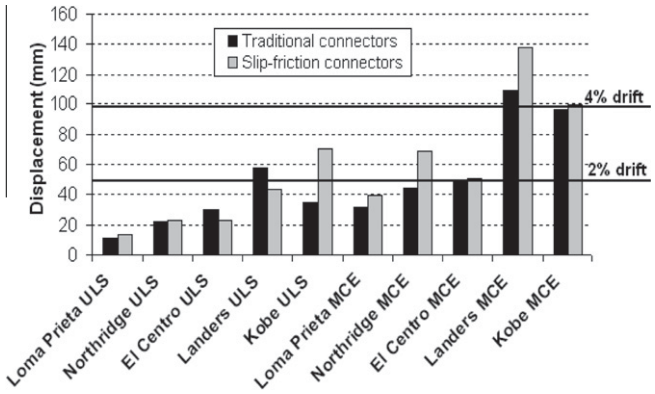

Fig. 14. Earthquake loading: maximum horizontal displacement at top of wall.

The Fast Nonlinear Analysis (FNA) method was used, with a time step of 0.01 s employed. The equivalent viscous damping was set to 1% for all considered modes of vibration.

4.2. Hysteretic behaviour

In Fig. 11, walls with traditional connectors are compared with walls with slip-friction connectors, for each earthquake event.

Under Loma Prieta ULS loading (see Fig. 11(a)) the wall with traditional connectors remained largely elastic. However under Landers and Kobe ULS loadings (see Figs. 11(e) and (i), respectively) the walls with traditional connectors incurred significant inelastic damage, as did walls under Northridge and El Centro ULS loadings (not presented here). In spite of this, all of these walls maintained strength levels at or above the yield strength of F_y = 8.4 kN, and none were displaced to failure.

The walls with slip-friction connectors performed as expected under ULS loading, producing square shaped hysteresis loops approximating ideal elasto-plastic behaviour. As was intended, base shear was generally capped to around 8.4 kN.

For MCE loading, walls with traditional connectors behaved differently under different earthquake events. For the Loma Prieta event (see Fig. 11(c)), Northridge, and El Centro events (not presented here), the walls all underwent significant inelastic material deformation, with the activated base shear approaching or just achieving the ultimate strength (16.7 kN) of the wall. However, under Landers and Kobe MCE loadings (see Figs. 11(g) and (k), respectively), the walls experienced rapid declines in strength and stiffness after ultimate strength had been achieved, and thus completely failed.

In the case of those walls with slip-friction connectors, all survived under MCE loading, with the force–displacement relationships exhibiting elasto-plastic behaviour similar to that observed for the same walls under ULS loading.

4.3. Forces on end-chords

Fig. 12 compares the peak tension forces in end-chords for walls with traditional connectors, against walls with slip-friction connectors. Similar results were observed for compression forces (not presented).

It can be clearly seen that the slip-friction connectors put an upper limit on tension and compression forces in the chords. The maximum forces on the end-chords differed little between ULS loading on the one hand and MCE loading on the other – attesting to the fact that slip-friction connectors can provide a consistently high level of protection to the walls against inelastic damage – even during extreme earthquake events.

In a manner very similar to that for the end-chords, it is found that under both ULS and MCE loadings, the slip-friction connectors effectively cap the stresses which are carried by the sheathing (not presented here).

4.4. Nail deformations

The lateral displacement of a nail connection, regardless of its ultimate strength, is an indicator of its progression towards yield and failure. In Fig. 13, the performance of nails (from the top corner

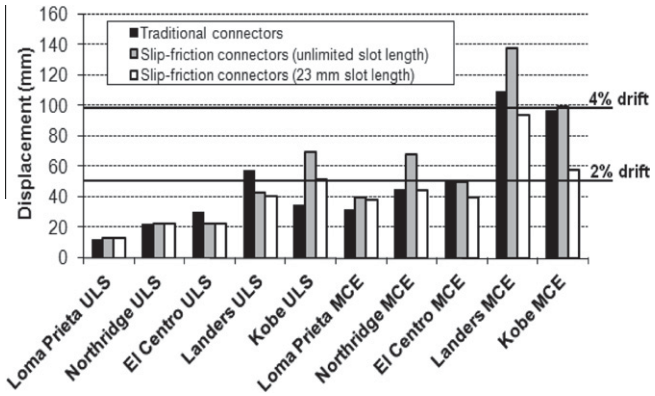

Fig. 15. Earthquake loading: maximum horizontal displacements at top of wall – the effect of restricting slot lengths.

of the wall) in walls with traditional connectors is compared with their performance in walls with slip-friction connectors.

For walls with slip-friction connectors under ULS loading, the nail displacements range from 1.3 to 1.5 mm. Under MCE loading, the nail displacements are not much larger, ranging from 1.4 to 1.6 mm.

Munoz et al. [14] reports an average yield displacement, from their experiments, of 1.5 mm for sheathing-to-wood nail connections (assuming F_y is 50% of F_{ult}). In this context, it can be seen from Fig. 13 that the nail connections in walls with slip friction connectors experience maximum displacements less than or equal to the yield displacement – except for the walls under Landers and Kobe MCE loadings. Both of these walls had maximum displacements of 1.6 mm.

This is in stark contrast to the effect of earthquake loading on the walls with traditional connectors. Under both ULS and MCE events (except for the Loma Prieta ULS case), nails experienced significant irrecoverable, inelastic deformations.

4.5. Displacements (unlimited connector slot lengths)

The maximum horizontal displacements of walls with slip-friction connectors are compared against those of walls with traditional connectors (Fig. 14).

If a 2% lateral drift level is considered the threshold under which there is minimal need of repair following an earthquake event, it can be seen that this criteria is met by all the walls with traditional connectors under ULS loading, except in the case of the Landers event. For walls with slip-friction connectors, except for the wall loaded by the Kobe event, low levels of horizontal displacement are also observed under ULS loading.

For the MCE events, walls with slip-friction connectors have higher displacements than walls with traditional connectors. In the case of the Northridge and Landers events the differences are significant. However, apart from the Landers event, maximum displacements for all walls, regardless of connector type, remain under a 4% drift level.

4.6. Displacements (limited connector slot lengths)

In light of the high drifts caused by the Kobe and Landers events (see Fig. 14) all the walls were considered again under the same loading, but with connector slot lengths set so that $\mu_{SF} = 4$. From the monotonic force–displacement envelope, as previously mentioned, the yield displacement $\delta_y = 7.6$ mm. From Eq. (5), the slot length is then calculated to be 23 mm.

The effect of limiting the connector slot length on wall displacement is shown in Fig. 15.

It can be seen that restricting slot lengths results in either zero change to maximum displacement (naturally so for those events in which the maximum displacements for walls with unrestricted slots was less than 23 mm), or a reduction in maximum displacement. The most significant result is for the Kobe MCE event, which shows a reduction in maximum wall displacement of almost 50%, simply through limiting the connector slot length. For walls under Kobe ULS, Landers MCE and Northridge MCE loadings, significant reductions in displacement due to limiting the connector slot length are also observed.

Thus it appears that under earthquake loading, walls with slip-friction connectors will experience a reduction in maximum displacement – if a limit is placed on connector slot length. However, this desirable outcome is offset by an increased likelihood of inelastic damage to the walls occurring. Inelastic damage occurs when the bolt of a slip-friction connector impacts against the slot end, and uncapped force is then transferred to the studs, sheathing, and nail connections of the wall. In the considered walls, this effect

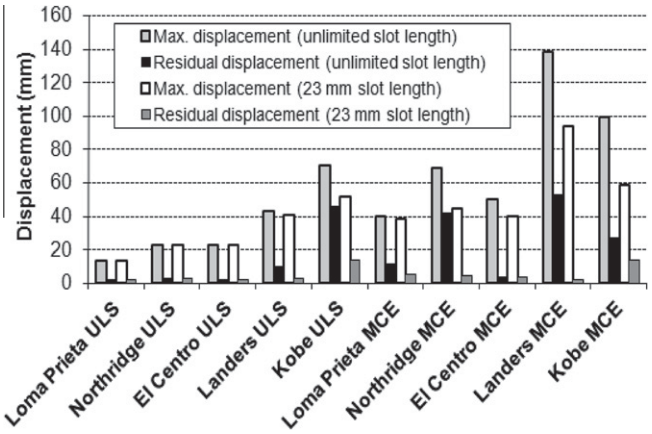

Fig. 16. Residual displacements compared with maximum displacements.

is particularly pronounced for the Landers MCE, Kobe ULS, and Kobe MCE events. However, it should be noted that even under these three earthquake events, in spite of the damage to the walls from limiting connector slot lengths to 23 mm, the walls did not suffer significant loss in strength at any point within the considered time window, and the maximum drift level was kept to below 4%. In the case of an MCE event, some damage can be expected, but the main performance requirement is that the wall is not deformed or displaced to the point where catastrophic collapse is imminent.

4.7. Self-centring

An important performance criterion of slip-friction connectors, is not only to avoid inelastic material damage and efficiently dissipate seismic energy during an earthquake, but also to allow the shear wall to self-centre immediately after the earthquake has ended. Factors that could influence how well a wall self-centres, include the nature of the dynamic load, the configuration of the wall itself, the inertial weight supported by the wall, and the vertical loads imposed on the wall.

Fig. 16 compares residual displacements after an earthquake event, with maximum displacements during the same earthquake event. This is done both for walls with slip-friction connectors of unlimited slot length, and for walls with slip-friction connectors of limited slot length (23 mm).

Whilst all the cases in Fig. 16 demonstrate that walls with slip-friction connectors have a strong tendency to self-centre, it is also clear that limiting slot lengths can significantly improve results. This is particularly the case for those walls loaded by the Kobe ULS, Kobe MCE, Northridge MCE, and Landers MCE events.

5. Conclusions

From this study, it is evident that there is the potential to significantly improve some aspects of the earthquake performance of timber walls by replacing traditional hold-down connectors with slip-friction connectors.

Cyclic loading has shown that slip-friction connectors can effectively cap stresses on shear walls, thereby protecting them from inelastic damage.

Under the considered earthquake loadings, the model walls with traditional hold-down connectors incurred significant inelastic damage. Replacing these hold-down connectors with slip-friction connectors enabled the same walls, under both design level and maximum considered earthquake loadings, to avoid significant inelastic deformations.

In general, under the same earthquake event, walls with slip-friction connectors did not experience drift levels significantly greater than those of walls with traditional connectors.

Walls with unrestricted slot lengths performed well with respect to post-earthquake self-centring – however this performance was further improved on by providing slip friction connectors with realistic slot lengths.

Further investigations are necessary to confirm the effectiveness of slip-friction connectors in a whole structure and to identify their limitations in practical application.

Acknowledgements

The authors would like to thank the New Zealand Ministry of Agriculture and Forestry for the support of this research, and the four anonymous reviewers for their constructive comments that have improved the clarity of this article.

References

[1] Banks W. Plywood shear walls – worked examples. NZ Timber Design Journal 2007;15(2):9–15.
[2] Judd JP, Fonseca FS. Analytical model for sheathing-to-framing connections in wood shear walls and diaphragms. J Struct Eng 2005;131(2):345–52.
[3] Bora C, Oliva M, Nakaki S, Becker R. Development of a unique precast shear wall system with special code acceptance. PCI J 2007;52(1):122–35.
[4] Popov E, Grigorian C, Yang T. Developments in seismic structural analysis and design. Eng Struct 1995;17(3):187–97.
[5] Clifton C, MacRae H, Mackinven S, Pampanin S, Butterworth J. Sliding hinge joints and subassemblies for steel moment frames. Palmerston North, New Zealand: Proc of New Zealand Society for Earthq Eng Conf; 2007.
[6] Butterworth J. Ductile concentrically braced frames using slotted bolted joints. J Struct Eng Society of New Zealand 2000;13(1):39–48.
[7] Filiatrault A. Analytical predictions of the seismic response of friction damped timber shear walls. Earthq Eng Struct Dyn 1990;19(2):259–73.
[8] Duff SF, Black R, Mahin S, Pampanin S, Blondet M. Friction-damped energy dissipating timber connections, vol. 1. Montreux, Switzerland: Proc of 5th World Conf on Timber Eng; 1998 [p. 361–368].
[9] Computers and Structures, Inc. SAP2000 v14: Integrated solution for structural analysis and design. California: Berkeley; 2009.
[10] Ayoub A. Seismic analysis of wood building structures. Eng Struct 2006;29(2):213–23.
[11] Blasetti AS, Hoffman R, Dinehart D. Simplified hysteretic finite-element model for wood and viscoelastic polymer connections for the dynamic analysis of shear walls. J Struct Eng 2008;134(1):77–86.
[12] Varoglu E, Karacabeyli E, Stiemer S, Ni C. Midply wood shear wall system: concept and performance in static and cyclic testing. J Struct Eng 2006;132(9):1417–25.
[13] NZS3603. Timber structures standard. Wellington, New Zealand: Standards New Zealand; 1993.
[14] Munoz W, Salenikovich A, Mohammad M, Quenneville P. Determination of yield point and ductility of timber assemblies: in search for a harmonised approach. Proc of Meeting 41 of CIB-W18. Canada: St Andrews; 2008.
[15] Pacific Earthquake Engineering Research Center (PEER). PEER strong motion database.<http://peer.berkeley.edu/smcat/>. [accessed 18.10.09].
[16] NZS1170. Structural design actions part 5: Earthquake actions. Wellington, New Zealand: Standards New Zealand; 2004.